Article

On the Effect of a Rate-Dependent Work of Adhesion in the Detachment of a Dimpled Surface

Antonio Papangelo [1,2] (ID)

1 Politecnico di BARI, Department of Mechanics, Mathematics and Management, Via Orabona 4, 70125 Bari, Italy; antonio.papangelo@poliba.it or antonio.papangelo@tuhh.de
2 Department of Mechanical Engineering, Hamburg University of Technology, Am Schwarzenberg Campus 1, 21073 Hamburg, Germany

Abstract: Patterned surfaces have proven to be a valuable design to enhance adhesion, increasing hysteresis and the detachment stress at pull-off. To obtain high adhesive performance, soft materials are commonly, used, which easily conform to the countersurface, such as soft polymers and elastomers. Such materials are viscoelastic; i.e., they show rate-dependent properties. Here, the detachment of two half spaces is studied, one being flat and the other having a dimple in the limit of short range adhesion and a power law rate-dependent work of adhesion, as observed by several authors. Literature results have suggested that the dimpled surface would show pressure-sensitive adhesion, showing two possible adhered states, one weak, in partial contact, and one strong when full contact is achieved. By accounting for a power law rate-dependent work of adhesion, the "weak state" may be much stronger than it was in the purely elastic case, and hence the interface may be much more tough to separate. We study the pull-off detachment stress of the dimpled surface, showing that it weakly depends on the preload, but it is strongly affected by the dimensionless unloading rate. Finally, possible implications of the presented results in the detachment of soft materials from rough substrates are discussed.

Keywords: adhesion enhancement; dimple model; patterned surfaces; viscoelasticity; enhancement

1. Introduction

Tribology is a very active field of research of utmost importance in several engineering applications, ranging from automotive [1] to aerospace [2] and bio-engineering [3]. In automotive, for example, the role of adhesion and viscoelasticity is crucial in determining tires' adherence and performance [4]. Adhesion due to van der Waals interactions is commonly exploited in nature, in which very efficient strategies have been developed to adhere to almost any kind of surface [5,6]. Lizardw, geckos and insects in general in most cases outperform the most advanced human designed adhesive technologies, and the topic still has far to go. Geckos for example have developed a multiscale hierarchical structure, so that the "macroscopic" foot splits in several lamellae, which branch in the setae and finally in fine spatulae of the size of nanometers [7,8]. Inspired by nature, several adhesive strategies have been pursued, among the others, that of fabricating patterned surfaces [9] present in mushroom pillars [10] or depressions ("dimples") [9] (see Figure 1a) and have been shown to be able to reach far higher adhesive stress with respect to the smooth case. Nevertheless, simple criteria to discern sticky from unsticky surfaces are still unavailable [11–13], except maybe the criterion introduced by Dalquist at 3M, who suggested that a strong adhesive tape should have a Young's modulus lower than 0.3 MPa to be able to conform well to the harder counterpart [14], which, only recently, has received some support from a theoretical perspective [11,12].

Over the years, several authors have conceived of contact mechanics models to ascertain how the enhancement is originated and possibly indicate routes for further development or better performance [15–17]. A very elegant model for the detachment of a

halfspace with a dimple from a flat substrate was proposed by McMeeking et al. [17], who developed a contact mechanics model in the limit of short range adhesion (the so-called "JKR limit" from Johnson, Kendall, and Roberts' seminal paper [18]) and showed that the dimple surface behaved as a pressure-sensitive adhesive: detaching the dimple from its equilibrium position would lead to "weak adhesion" in partial contact, but upon application of a compressive pressure, a full-contact state would be achieved that would require a (theoretically) infinite tensile traction to be detached ("strong adhesion"). In this respect, the finding recalls the seminal work of Johnson [19], who considered the contact of a halfplane with sinusoidal waviness. Johnson had to postulate the presence of a flaw at the interface (air trapping, contaminants, fine scale roughness...), which would guarantee the possibility to separate the two surfaces. Zhou et al. [15] have applied the McMeeking et al. [17] model to study the adhesion capabilities of both cockroach pads (*Nauphoeta cinerea*) and dock beetles pads (*Gastrophysa viridula*), showing that they are strongly influenced by the geometric features of the interfacial pattern, and Cañas et al. [20] adopted the McMeeking et al. [17] model to fit experimental results of adhesion of biomimetic polydimethylsiloxane (PDMS) surfaces patterned with pillars with mushroom-shaped tips.
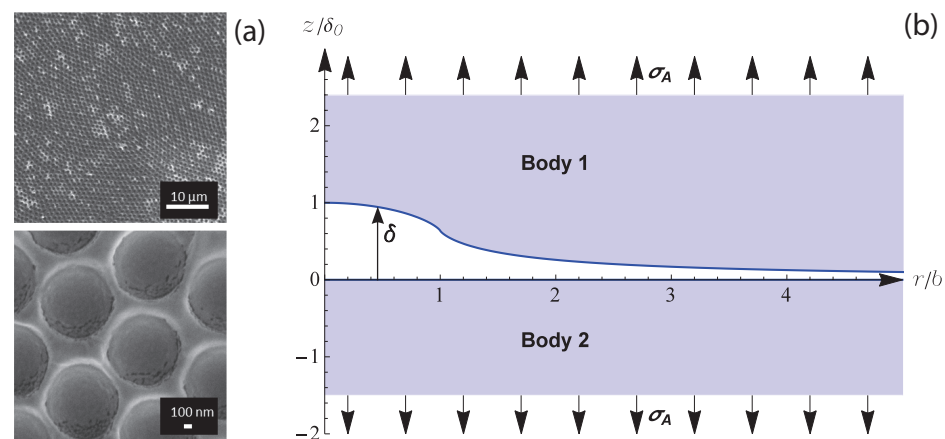

Figure 1. (**a**) SEM images of a surface pattered with dimples (adapted from [9]). (**b**) Geometry of the dimple surface considered in this study. The model is axysimmetric.

Recently, Papangelo and Ciavarella [21] generalized the "dimple" model of McMeeking et al. [17] by using a cohesive Maugis–Dugdale model, which introduces two new parameters, i.e., the theoretical strength of the material and the range of interaction of the adhesive tractions, and allowed investigation of the detachment performance of the dimple ranging from soft to hard materials as a function of a dimensionless parameter that is similar to that introduced by Tabor for the sphere [21,22]. It was shown that the dimple adhesive performance, particularly the "strong adhesive state", becomes rapidly degraded, moving towards the rigid limit; hence for the dimple to effectively work as a pressure-sensitive mechanism, soft materials should be employed.

The above studies have considered the work of adhesion (the work needed to separate two flat surfaces from their equilibrium position up to infinity) as a constant that depends on the contact pair. Nevertheless, it is well-known that soft materials show rate-dependent properties. In particular, the dependence of the work of adhesion w on the velocity of the peeling v_p (the velocity at the crack tip) is well documented both experimentally [23,24] and theoretically [25,26]. Although with some variants in the nomenclature, most of the authors agree that the dependence of the work of adhesion on the peeling velocity is well captured by a power law form (Reference [27])

$$w = w_0 \left[1 + \left(\frac{v_p}{V_0} \right)^n \right]$$

(1)

where w_0 is the adiabatic (or thermodynamic) work of adhesion for vanishing peeling velocity, while V_0 and n are material properties with V_0 a reference velocity, and n an exponent usually in a range from 0.1 to 0.9 for realistic materials. Here, we revise the model of McMeeking et al. [17] by accounting for the effect of the rate at which the external load is applied. It will be shown that the dimple still behaves as a pressure-sensitive adhesive, but the "weak" adhesive state is strongly influenced by the unloading rate so that the pull-off stress in partial contact and the interfacial toughness can largely increase for high unloading velocity. The enhancement effect is greatly dependent on the exponent n, larger exponents leading to larger strengthening of the interface, but it is only marginally affected by the level of preload.

2. Griffith Equilibrium Solution for a Dimple

2.1. Elastic Problem

Here, the model introduced by McMeeking et al. [17] for the detachment of two elastic half-spaces is summarized. The geometry consists of two elastic bodies (see Figure 1b), with Young's modulus and Poisson's ratio $\{E_1, \nu_1\}$ and $\{E_2, \nu_2\}$, one of those flat while the other with an axysimmetric dimple, whose geometry is defined by (see Figure 1b)

$$\begin{cases} \delta = \frac{2}{\pi}\delta_0\varepsilon\left(\frac{r}{b}\right), & \frac{r}{b} \leq 1 \\ \delta = \frac{2r}{\pi b}\delta_0\left[\varepsilon\left(\frac{b}{r}\right) - \left(1 - \frac{b^2}{r^2}\right)\kappa\left(\frac{b}{r}\right)\right], & \frac{r}{b} > 1 \end{cases} \qquad (2)$$

where r is the radial coordinate, δ_0 is the dimple amplitude, b is the dimple radius, $\kappa(\theta)$ and $\varepsilon(\theta)$ are, respectively, the complete elliptical integral of first and second kind with argument θ. Johnson [28] has shown that a uniform axisymmetric pressure of magnitude p applied over a region $r < b$ on the surface of a half-space produces surface displacements as in Equation (2); hence, to make the two half-spaces conform to each other, one would need within the dimple ($r \leq b$) a tensile traction T equal to [28]

$$T = \frac{E^*\delta_0}{2b}, \qquad r \leq b \qquad (3)$$

where $\frac{1}{E^*} = \frac{1-\nu_1^2}{E_1} + \frac{1-\nu_2^2}{E_2}$ is the composite elastic modulus. Hence, if a remote stress σ_A (>0, when tensile) is applied, the stress σ_{zz} at the interface of the two half-spaces will be

$$\begin{cases} \sigma_{zz} = \sigma_A + \frac{E^*\delta_0}{2b}, & \frac{r}{b} \leq 1 \\ \sigma_{zz} = \sigma_A, & \frac{r}{b} > 1 \end{cases} \qquad (4)$$

The combination of the remote stress applied and the inner (constant) stress within the dimple can be easily studied in the framework of the Linear Elastic Fracture Mechanics (LEFM) theory, as the dimple behaves as an axisymmetric crack under internal pressure $p(r)$ [29]. Let us define, for a crack of radius c, the auxiliary function ([29], 3.114a) $g(x) = \int_0^x \frac{sp(s)ds}{\sqrt{x^2-s^2}}$

$$\begin{cases} g(x) = (\sigma_A + T)x, & x < b \\ g(x) = \sigma_A x + T\left(x - \sqrt{x^2 - b^2}\right), & x > b \end{cases} \qquad (5)$$

Then, Equation (3.117) in [29] gives the stress intensity factor as $K_I = \frac{2}{\sqrt{\pi c}}g(c)$, or equivalently, the energy release per unit area $G = K_I^2/2E^*$

$$\begin{cases} G = \frac{2c}{\pi E^*}\left(\sigma_A + \frac{E^*\delta_0}{2b}\right)^2, & \frac{c}{b} \leq 1 \\ G = \frac{2c}{\pi E^*}\left[\sigma_A + \frac{E^*\delta_0}{2b}\left(1 - \sqrt{1 - \left(\frac{b}{c}\right)^2}\right)\right]^2 & \frac{c}{b} > 1 \end{cases} \qquad (6)$$

Hence McMeeking et al. [17] apply the classical Griffith energetic argument that the energy release per unit area G should be equal to the surface energy w_0 of the contact pair

(the "toughness"), leading to their LEFM model [17]. The equilibrium curves that link the remote tension to the crack radius are written in dimensionless form as

$$
\begin{cases}
\widehat{\sigma}_A = -1 + \alpha_d \sqrt{\frac{1}{\widehat{c}}}, & \widehat{c} \leq 1 \\
\widehat{\sigma}_A = -1 + \alpha_d \sqrt{\frac{1}{\widehat{c}}} + \sqrt{1 - \left(\frac{1}{\widehat{c}}\right)^2}, & \widehat{c} > 1
\end{cases}
\tag{7}
$$

where we have introduced the following dimensionless parameters

$$
\alpha_d^2 = \frac{2\pi w_0 b}{E^* \delta_0^2}, \qquad \widehat{\sigma}_A = \frac{\sigma_A}{T}, \qquad \widehat{c} = \frac{c}{b},
\tag{8}
$$

Notice that α_d is analogous to the parameter that Johnson defined for the sinusoid [28] as it is proportional to the ratio between the adiabatic work of adhesion and the strain elastic energy to flatten the dimple. Figure 2 shows the equilibrium solutions for $\alpha_d = [0.1, 0.5, 0.9]$, where we used a solid (dashed) line to identify the stable (unstable) branches of the curve. For the curve $\alpha_d = 0.5$, we have labelled some noteworthy points. The system is in equilibrium under vanishing remote stress $\widehat{\sigma}_A = 0$ at the point "C", which corresponds also to a certain radius (not null) of the crack $\widehat{c}$. If a tensile stress is applied, the crack radius increases and detachment takes place at point "B" in partial contact (Reference [21] reports $\widehat{c}$ at pull-off), which will be referred to as the "weak" adhered state. If, from the equilibrium position "C", a compressive pressure is applied below $\widehat{\sigma}_{A,C} = -1 + \alpha_d$, the dimple jumps from point "A" to a full contact state (the branch below $\widehat{c} = 1$ is unstable); hence, the crack shrinks, and theoretically an infinite tensile pressure will be needed to separate the two bodies. In practice, there may be flaws, contaminants, air trapping or simply the two surfaces will be detached when the theoretical strength is reached (see [21] for a detailed analysis).
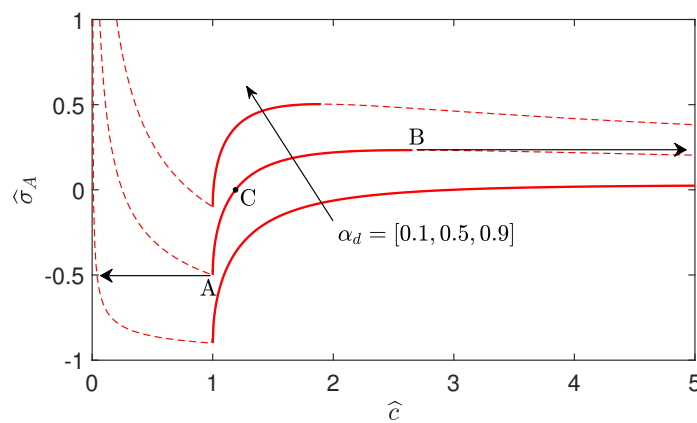

Figure 2. Remote stress $\widehat{\sigma}_A$ versus the crack radius $\widehat{c}$ in the McMeeking et al. [17] elastic model for $\alpha_d = [0.1, 0.5, 0.9]$. For the curve $\alpha_d = 0.5$, point "C" determines the equilibrium position ($\widehat{\sigma}_A = 0$), point "B" the "weak" adhesive state, while point A is the point where the jump to full contact happens.

2.2. Effect of a Rate-Dependent Work of Adhesion

We have introduced above the McMeeking et al. [17] LEFM elastic model for the detachment a dimpled half-space from a flat substrate. Nevertheless, soft matter has viscoelastic behavior; hence, we here extend the McMeeking et al. [17] model to account for a rate-dependent work of adhesion. According to Equation (1), the effective work of adhesion is a power-law function of the peeling velocity $v_p = dc/dt$ (t is the time), i.e., the velocity at the crack tip, which can be written as

$$
v_p = \frac{dc}{dt} = \pm\dot{\sigma}_A \frac{dc}{d\sigma_A}
\tag{9}
$$

where $\dot{\sigma}_A = d\sigma_A/dt$ [Pa/s] is the externally imposed unloading rate and the "+" ("−") sign holds when the crack advances ($dc/dt > 0$) or retracts ($dc/dt < 0$). Hence, using (1), (6) and (9) and imposing the Griffith equilibrium concept, one obtains

$$
\begin{cases}
w_0 \left[1 + \left(-\frac{\dot{\sigma}_A}{V_0} \frac{dc}{d\sigma_A} \right)^n \right] = \frac{2c}{\pi E^*} \left(\sigma_A + \frac{E^* \delta_0}{2b} \right)^2, & \frac{c}{b} \leq 1 \\[4mm]
w_0 \left[1 + \left(\frac{\dot{\sigma}_A}{V_0} \frac{dc}{d\sigma_A} \right)^n \right] = \frac{2c}{\pi E^*} \left[\sigma_A + \frac{E^* \delta_0}{2b} \left(1 - \sqrt{1 - \left(\frac{b}{c}\right)^2} \right) \right]^2, & \frac{c}{b} > 1
\end{cases}
\tag{10}
$$

which in dimensionless notation reads

$$
\begin{cases}
\frac{d\hat{c}}{d\hat{\sigma}_A} = -\frac{1}{\dot{\hat{\sigma}}_A} \left[\frac{\hat{c}}{\alpha_d^2} (\hat{\sigma}_A + 1)^2 - 1 \right]^{1/n}, & \hat{c} \leq 1 \\[4mm]
\frac{d\hat{c}}{d\hat{\sigma}_A} = \frac{1}{\dot{\hat{\sigma}}_A} \left\{ \frac{\hat{c}}{\alpha_d^2} \left[\hat{\sigma}_A + \left(1 - \sqrt{1 - \frac{1}{\hat{c}^2}} \right) \right]^2 - 1 \right\}^{1/n}, & \hat{c} > 1
\end{cases}
\tag{11}
$$

where the dimensionless unloading rate $\dot{\hat{\sigma}}_A = \frac{\dot{\sigma}_A}{TV_0/b}$ has been introduced. The ordinary differential equations in (11) are of first order and can be easily solved numerically using as a starting point a solution of the elastic problem in Equation (7). Clearly, physically admissible starting points are those on the stable branch AB in Figure 2; hence, as we shall see later, a rate-dependent work of adhesion will not affect the "strong" adhesive state, but only the "weak" one. In the next section we shall investigate the effects of the various parameters $\left\{ n, \dot{\hat{\sigma}}_A, \alpha_d \right\}$ on the detachment stress in partial contact ("weak" state).

3. Results

3.1. Detachment Curves

Let us investigate first the effect that a rate-dependent work of adhesion has on the detachment curve of the dimple by solving Equation (11). Figure 3 shows the unloading curves for the rate-dependent model (Equation (11), black dot-dashed curves) starting from different initial conditions $\hat{c}_0$ on the branch AB (Figure 2) for $\alpha_d = 0.5$, $n = 0.5$ and $\dot{\hat{\sigma}}_A = 1$. The red curve (solid for the stable, dashed for the unstable branches) shows the Griffith elastic reference solution [17]. Clearly, the rate-dependence of the work of adhesion has a toughening effect (dot-dashed black curves). Figure 4a shows the dimensionless peeling velocity $\hat{v}_p = v_p/V_0$ as it changes during the detachment process, while panel (b) shows the corresponding dimensionless work of adhesion $\hat{w} = w/w_0$, while the crack propagates. The peeling process starts with a vanishing velocity; i.e., instantaneously, the remote stress increases without change of the crack radius $\hat{c}$, and this can be easily checked if one substitutes a solution of the Griffith elastic model (Equation (7)) into the rate-dependent model (Equation (11)). By further unloading the dimple surface $\left(\dot{\hat{\sigma}}_A > 0 \right)$, the peeling velocity $\hat{v}_p$ increases with a power law behavior, and so does the interfacial toughness. Notice that the slope of the $\hat{\sigma}_A(\hat{c})$ curve is inversely proportional to the peeling velocity; hence, the latter decays with a power law. We define the pull-off detachment stress as $\hat{\sigma}_{A,pull} = \lim_{\hat{c} \to +\infty} \hat{\sigma}_A$. Furthermore, Figure 3 shows the crack retraction curve, when the dimple is forced into the unstable regime ($\hat{c} \leq 1$, blue dot-dashed curve). Apart from a different transient behavior, similarly to the elastic solution, the rate-dependent solution will jump into a full contact strong adhesive state. Figure 3 shows that the effect of the initial preload on the detachment stress $\hat{\sigma}_{A,pull}$ is marginal, particularly in light of the dependencies on the parameters $\left\{ n, \dot{\hat{\sigma}}_A, \alpha_d \right\}$ that we will show in the following. From now on, we will consider as initial condition only the more "likely" situation of unloading the dimple from its equilibrium position $\hat{\sigma}_A = 0$, which belongs to the stable branch AB

for $\alpha_d \leq 1$ (otherwise for $\alpha_d > 1$, the dimple naturally jumps into the full-contact strong adhesive state).
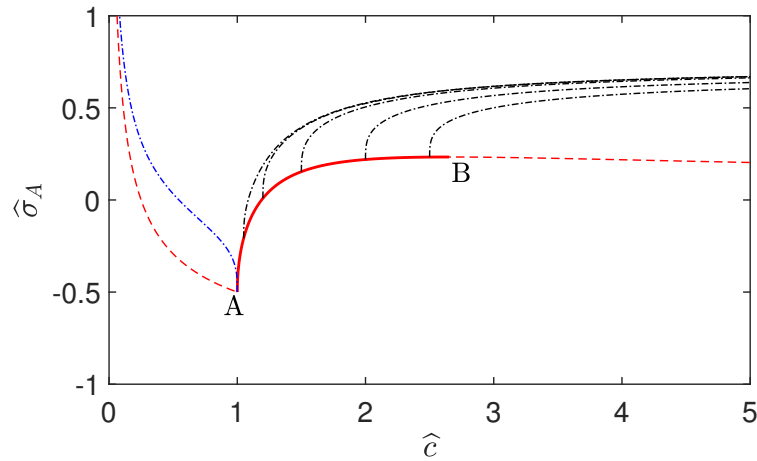

Figure 3. Unloading curves of the dimpled surface starting from different initial conditions $\hat{c}_0 = [1.05, 1.2, 1.5, 2, 2.5]$ for $\alpha_d = 0.5$, $n = 0.5$ and $\dot{\hat{\sigma}}_A = 1$. Red lines for the Griffith elastic solution, dot-dashed black lines for the rate-dependent model unloading curves.
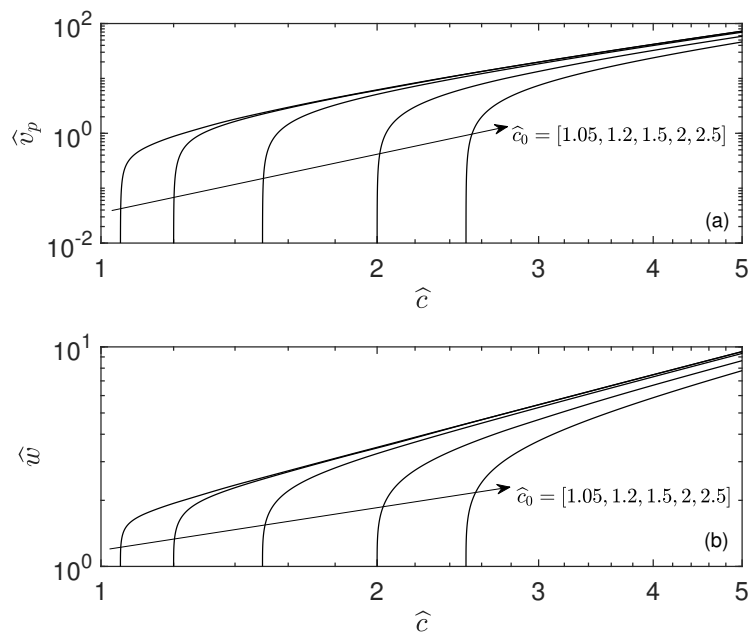

Figure 4. (**a**) Dimensionless peeling velocity and (**b**) corresponding apparent work of adhesion $\hat{w} = w/w_0$ for the unloading curves in Figure 3.

Let us look at the influence of the exponent n and of the unloading rate $\dot{\hat{\sigma}}_A$ on the dimple detachment curves. Figure 5a shows that starting from the dimple equilibrium position "C" for $\alpha_d = 0.5$, $n = 0.5$ and $\dot{\hat{\sigma}}_A = 10^{[-3,0,1,2]}$, where black dot-dashed curves indicate the rate-dependent solutions, while the red curves show the reference elastic solution. Figure 5a shows that the unloading rate has a strong influence on the detachment stress $\hat{\sigma}_{A,pull}$ and that the elastic solution is approached only for the very low unloading rate $\dot{\hat{\sigma}}_A = 10^{-3}$. Notice that, in this particular case, for the reference elastic solution, we have $\hat{\sigma}_A|_{max} \approx 0.23$,, while in the a rate-dependent case $\hat{\sigma}_{A,pull} \approx 1.7$ at $\dot{\hat{\sigma}}_A = 10^2$,

which gives a detachment stress increased by a factor $\simeq 7$. Finally panel (b) shows that for the same unloading rate $\dot{\hat{\sigma}}_A = 1$, the pull-off stress $\hat{\sigma}_{A,pull}$ increases with the exponent $n = [0.1, 0.3, 0.5, 0.7, 0.9]$ as for the increasing of the effective surface energy w (see Equation (1)).
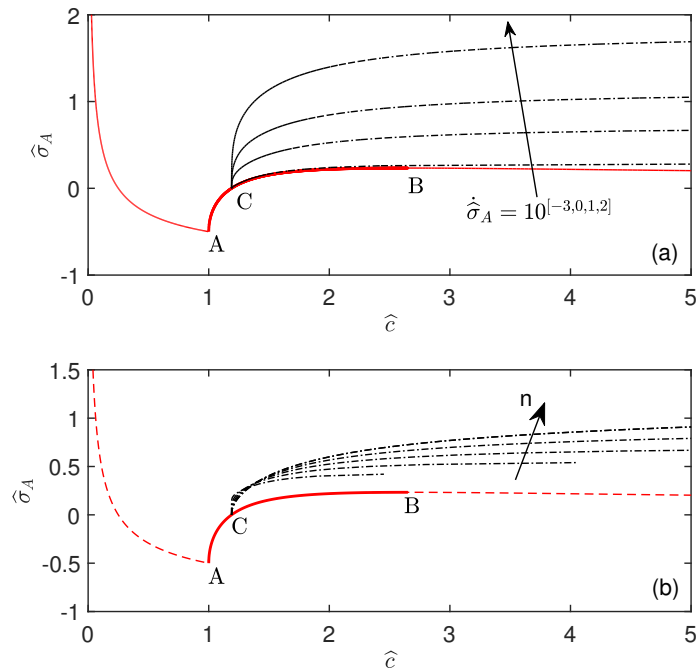

Figure 5. (**a**) Unloading curves of the dimpled surface starting from $\hat{\sigma}_A = 0$ for $\alpha_d = 0.5$, $n = 0.5$ and $\dot{\hat{\sigma}}_A = 10^{[-3,0,1,2]}$. Red lines for the Griffith elastic solution, dot-dashed black lines for the a rate-dependent unloading curves. (**b**) As panel (**a**) but for $\dot{\hat{\sigma}}_A = 1$ and $n = [0.1, 0.3, 0.5, 0.7, 0.9]$.

3.2. Pull-Off Detachment Stress

We have investigated the effect of the unloading rate $\dot{\hat{\sigma}}_A$ and of the exponent n on the detachment curves of a dimple from an elastic substrate with rate-dependent work of adhesion. Here we give a closer look at the dependence of the pull-off stress $\hat{\sigma}_{A,pull}$ on the unloading rate $\dot{\hat{\sigma}}_A$ by varying α_d and n. Figure 6a shows the pull-off stress $\hat{\sigma}_{A,pull}$ as a function of the dimensionless unloading rate $\dot{\hat{\sigma}}_A$ for $\alpha_d = [0.2, 0.4, 0.6, 0.8]$ and $n = 0.5$. Panel (a) shows that the the pull-off stress $\hat{\sigma}_{A,pull}$ approaches the elastic value (obtained from Equation (7)) only at very low unloading rate $\dot{\hat{\sigma}}_A \approx 10^{-4}$, while it increases considerably when $\dot{\hat{\sigma}}_A$ is increased, or by increasing α_d. In the regime of high unloading rate, the pull-off stress dependence on $\dot{\hat{\sigma}}_A$ is well captured by a power law behavior, while that on α_d is linear. For $\dot{\hat{\sigma}}_A \gtrsim 10^{-2}$ and $n = 0.5$, a very good fit of the pull-off stress is given by the power law

$$\hat{\sigma}_{A,pull} = (1.32\alpha_d + 0.065)\dot{\hat{\sigma}}_A^{0.2} \tag{12}$$

whose predictions are given by dot-dashed black lines (almost indistinguishable from the solid curves obtained numerically). Panel (b) shows that for a fixed $\alpha_d = 0.5$, the pull-off stress increases with the exponent n. At low $\dot{\hat{\sigma}}_A$, all the curves start from the same elastic solution (black dashed lines) as the pull-off stress depends only on α_d and then increases for larger unloading rates with a power law behavior whose slope is very well fitted by

a power law $\widehat{\sigma}_{A,pull} \propto \dot{\widehat{\sigma}}_A{}^{0.3n+0.05}$. (For $\dot{\widehat{\sigma}}_A \gtrsim 10^{-2}$, an estimate of the pull-off stress as a function of α_d and n can be obtained by $\widehat{\sigma}_{A,pull} = 2n(1.32\alpha_d + 0.065)\dot{\widehat{\sigma}}_A{}^{0.3n+0.05}$, where we found this to be more accurate close to $n \approx 0.5$ and $\alpha_d = 0.5$.) Notice that typically $0 < n < 1$; hence, the increase of the pull-off stress with the unloading rate is sublinear.
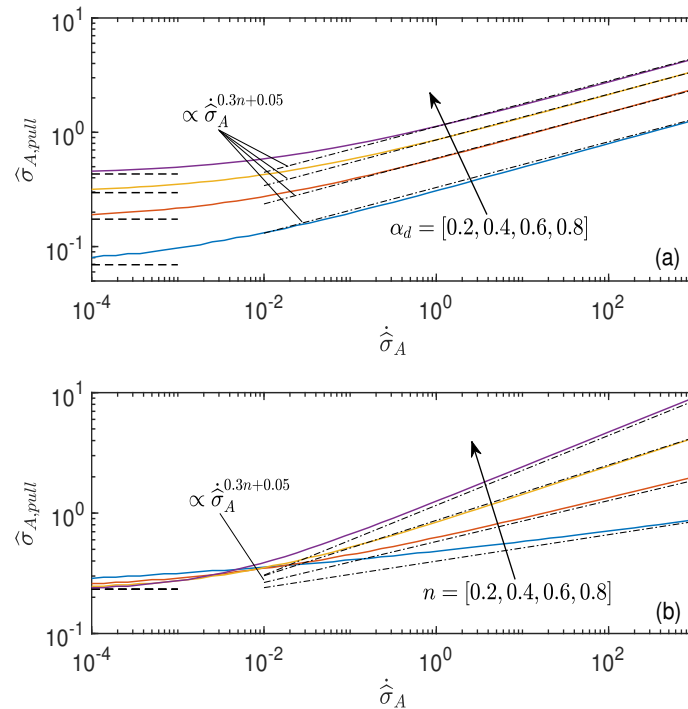

Figure 6. (**a**) Pull-off detachment stress $\widehat{\sigma}_{A,pull}$ as a function of the dimensionless unloading rate $\dot{\widehat{\sigma}}_A$ for $\alpha_d = [0.2, 0.4, 0.6, 0.8]$ and $n = 0.5$. (**b**) Pull-off detachment stress $\widehat{\sigma}_{A,pull}$ as a function of the dimensionless unloading rate $\dot{\widehat{\sigma}}_A$ for $n = [0.2, 0.4, 0.6, 0.8]$, $\alpha_d = 0.5$. For all the curves, the initial condition is $\widehat{\sigma}_A = 0$. In both panels, the black dashed lines indicate the Griffith equilibrium solution from Equation (7). Black dot-dashed lines serve as a guide to the eye.

4. Conclusions

In this work, the detachment of a surface with an axisymmetric dimple from an elastic substrate with rate-dependent work of adhesion has been studied in the limit of short-range adhesion. Previous elastic model with constant work of adhesion has shown that the dimpled surface has two adhered states, one "strong" in full contact, one "weak" in partial contact. The rate dependence of the work of adhesion has been accounted for by adopting a power law dependence (with exponent *n*) of the effective work of adhesion on the pealing velocity as it is commonly observed in experiments [27]. Notice that, in this analysis, we have neglected bulk effects (we used the relaxed modulus of the viscoelastic material $E_0 = E_{\omega=0}$, with ω being the excitation frequency of the material); hence, the results presented should be representative for not too high peeling velocity. It has been shown that a rate-dependent work of adhesion does not affect the "strong" adhesive state, but it strongly influences the detachment pull-off stress in partial contact, resulting in a strong toughening of the interface. In this respect, we have shown that for a given unloading rate, after a transient, the peeling velocity increases with a power law behavior during the detachment process, and so does the effective work of adhesion. Furthermore, it has been shown that the pull-off stress (in partial contact) does not depend much on the particular initial condition chosen to unload the dimple. Instead, the pull-off stress depends on three dimensionless parameters; i.e., it increases by increasing the unloading rate, the

exponent "n" or the dimensionless parameter α_d. Clearly, for a real viscoelastic material, the interfacial toughening will not increase to infinity but will be limited by the ratio $E_{\omega=\infty}/E_{\omega=0}$, which is known to vary anyway by orders of magnitude with the excitation frequency [26]. In this respect, for a real material, the curves in Figure 4 will be bounded. In conclusion, the presented results suggest that viscoelasticity may play a strong role in determining the apparent interfacial toughness in patterned interfaces. In particular, when soft rough substrates are considered, it may be very difficult to recognize other sources of toughening, such as those due to the increase of contact area due to roughness [30] or due the local jump instabilities as in the Guduru problem [31], unless an extremely low unloading rate is adopted as indeed recently attempted by Dalvi and coauthors [32].

Institutional Review Board Statement: Not applicable.

Informed Consent Statement: Not applicable.

Data Availability Statement: Not applicable.

Conflicts of Interest: The author declares no conflict of interest.

References

1. Hong, S.; Erdogan, G.; Hedrick, K.; Borrelli, F. Tyre–road friction coefficient estimation based on tyre sensors and lateral tyre deflection: Modelling, simulations and experiments. *Veh. Syst. Dyn.* **2013**, *51*, 627–647.
2. Yu, P.; Zhang, D.; Ma, Y.; Hong, J. Dynamic modeling and vibration characteristics analysis of the aero-engine dual-rotor system with Fan blade out. *Mech. Syst. Signal Process.* **2018**, *106*, 158–175. [CrossRef]
3. Li, X.; Tao, D.; Lu, H.; Bai, P.; Liu, Z.; Ma, L.; Tian, Y. Recent developments in gecko-inspired dry adhesive surfaces from fabrication to application. *Surf. Topogr. Metrol. Prop.* **2019**, *7*, 023001. [CrossRef]
4. Genovese, A.; Farroni, F.; Papangelo, A.; Ciavarella, M. A discussion on present theories of rubber friction, with particular reference to different possible choices of arbitrary roughness cutoff parameters. *Lubricants* **2019**, *7*, 85. [CrossRef]
5. Ciavarella, M.; Joe, J.; Papangelo, A.; Barber, J.R. The role of adhesion in contact mechanics. *J. R. Soc.* **2019**, *16*, 20180738. [CrossRef]
6. Kamperman, M.; Kroner, E.; del Campo, A.; McMeeking, R.M.; Arzt, E. Functional adhesive surfaces with "gecko" effect: The concept of contact splitting. *Adv. Mater.* **2010**, *12*, 335–348. [CrossRef] [PubMed]
7. Huber, G.; Gorb, S.; Hosoda, N.; Spolenak, R.; Arzt, E. Influence of surface roughness on gecko adhesion. *Acta Biomater* **2007**, *3*, 607–610. [CrossRef]
8. Pugno, N.M.; Lepore, E. Observation of optimal gecko's adhesion on nanorough surfaces. *Biosystems* **2008**, *94*, 218–222. [CrossRef]
9. Akerboom, S.; Appel, J.; Labonte, D.; Federle, W.; Sprakel, J.; Kamperman, M. Enhanced adhesion of bioinspired nanopatterned elastomers via colloidal surface assembly. *J. R. Interface* **2015**, *12*, 20141061. [CrossRef] [PubMed]
10. Paretkar, D.; Kamperman, M.; Martina, D.; Zhao, J.; Creton, C.; Lindner, A.; Arzt, E. Preload-responsive adhesion: Effects of aspect ratio, tip shape and alignment. *J. R. Soc.* **2013**, *10*, 20130171. [CrossRef] [PubMed]
11. Violano, G.; Afferrante, L.; Papangelo, A.; Ciavarella, M. On stickiness of multiscale randomly rough surfaces. *J. Adhesion* 2019, 1–19. [CrossRef]
12. Ciavarella, M. Universal features in "stickiness" criteria for soft adhesion with rough surfaces. *Tribol. Int.* **2020**, *146*, 106031. [CrossRef]
13. Tiwari, A.; Wang, J.; Persson, B.N.J. Adhesion paradox: Why adhesion is usually not observed for macroscopic solids. *Phys. Rev. E* **2020**, *102*, 042803. [CrossRef]
14. Dahlquist, C.A. *Treatise on Adhesion and Adhesives*; Patrick, R.L., Ed.; Marcel Dekker: New York, NY, USA, 1969; p. 244. [CrossRef] [PubMed]
15. Zhou, Y.; Robinson, A.; Steiner, U.; Federle, W. Insect adhesion on rough surfaces: Analysis of adhesive contact of smooth and hairy pads on transparent microstructured substrates. *J. R. Interface* **2014**, *11*, 20140499.
16. Kern, M.D.; Qi, Y.; Long, R.; Rentschler, M.E. Characterizing adhesion between a micropatterned surface and a soft synthetic tissue. *Langmuir* **2017**, *33*, 854–864. [CrossRef]
17. McMeeking, R.M.; Ma, L.; Arzt, E. Bi-Stable Adhesion of a Surface with a Dimple. *Adv. Eng. Mater.* **2010**, *12*, 389–397. [CrossRef]
18. Johnson, K.L.; Kendall, K.; Roberts, A.D. Surface energy and the contact of elastic solids. *Proc. R. Soc. Lond. A* **1971**, *324*, 1558. [CrossRef]

19. Johnson, K.L. The adhesion of two elastic bodies with slightly wavy surfaces. *Int. Solids Struct.* **1995**, *32*, 423–430.
20. Cañas, N.; Kamperman, M.; Völker, B.; Kroner, E.; McMeeking, R.M.; Arzt, E. Effect of nano-and micro-roughness on adhesion of bioinspired micropatterned surfaces. *Acta Biomater.* **2012**, *8*, 282–288. [CrossRef]
21. Papangelo, A.; Ciavarella, M. A Maugis–Dugdale cohesive solution for adhesion of a surface with a dimple. *J. R. Soc. Interface* **2017**, *14*, 20160996. [CrossRef]
22. Tabor, D. Surface forces and surface interactions. *J. Colloid Interface Sci.* **1977**, *58*, 2. [CrossRef]
23. Waters, J.F.; Guduru, P.R. Mode-mixity-dependent adhesive contact of a sphere on a plane surface. *Proc. R. A Math. Phys. Eng. Sci.* **2010**, *466*, 1303–1325. [CrossRef]
24. Barquins, M.; Maugis, D.; Blouet, J.; Courtel, R. Contact area of a ball rolling on an adhesive viscoelastic material. *Wear* **1978**, *51*, 375–384. [CrossRef]
25. Greenwood, J.A.; Johnson, K.L. The mechanics of adhesion of viscoelastic solids. *Philos. Mag. A* **1981**, *43*, 697–711. [CrossRef]
26. Persson, B.N.J.; Brener, E.A. Crack propagation in viscoelastic solids. *Phys. Rev. E* **2005**, *71*, 036123. [CrossRef]
27. Gent, A.N.; Schultz, J. Effect of wetting liquids on the strength of adhesion of viscoelastic material. *J. Adhes.* **1972**, *3*, 281–294. [CrossRef] [PubMed]
28. Johnson, K.L. *Contact Mechanics*; Cambridge University Press: Cambridge, UK, 1985. [CrossRef]
29. Maugis, D. *Contact, Adhesion and Rupture of Elastic Solids (Volume 130)*; Springer: New York, NY, USA, 2000.
30. Persson, B.N.J.; Tosatti, E. The effect of surface roughness on the adhesion of elastic solids. *J. Chem. Phys.* **2001**, *115*, 5597–5610.
31. Guduru, P.R. Detachment of a rigid solid from an elastic wavy surface: Theory. *J. Mech. Phys. Solids* **2007**, *55*, 473–488 [CrossRef]
32. Dalvi, S.; Gujrati, A.; Khanal, S.R.; Pastewka, L.; Dhinojwala, A.; Jacobs, T.D. Linking energy loss in soft adhesion to surface roughness. *Proc. Natl. Acad. Sci. USA* **2019**, *116*, 25484–25490. [CrossRef]